Pesticide Biochemistry and Physiology 186 (2022) 105152

Contents lists available at ScienceDirect

Pesticide Biochemistry and Physiology

journal homepage: www.elsevier.com/locate/pest

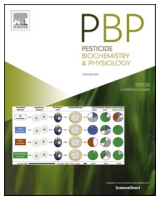

PharmacoGenetic targeting of *a C. elegans* essential neuron *provides* an in vivo screening for novel modulators of nematode ion channel function

Fernando Calahorro *, Mark Chapman, Katarzyna Dudkiewicz, Lindy Holden-Dye, Vincent O'Connor

School of Biological Sciences, University of Southampton, Life Sciences Building 85, Southampton SO17 1BJ, UK

ARTICLE INFO

Keywords:
Pharyngeal function
Monoxenic culture
5-HT
Quipazine
Cys-loop receptors
MOD-1
Ligand-gated chloride channel

ABSTRACT

Chemical or drug treatments are successfully used to treat parasitic nematode infections that impact human, animal and plant health. Many of these exert their effects through modifying neural function underpinning behaviours essential for parasite viability. Selectivity against the parasite may be achieved through distinct pharmacological properties of the parasite nervous system, as exemplified by the success of the ivermectin which target a glutamate-gated chloride channel found only in invertebrates. Despite the success of the ivermectins, emerging resistance and concerns around eco-toxicity are driving the search for new nematocidal chemicals or drugs. Here, we describe the potential of a 5-HT-gated chloride channel MOD-1, which is involved in vital parasite behaviours with constrained distribution in the invertebrate phyla. This ion channel has potential pharmacophores that could be targeted by new nematocidal chemicals and drugs. We have developed a microtiter based bioassay for MOD-1 pharmacology based on its ectopic expression in the *Caenorhabditis elegans* essential neuron M4. We have termed this technology 'PhaGeM4' for 'Pharmacogenetic targeting of M4 neuron'. Exposure of transgenic worms harbouring ectopically expressed MOD-1 to 5-HT results in developmental arrest. By additional expression of a fluorescence marker in body wall muscle to monitor growth we demonstrate that this assay is suitable for the identification of receptor agonists and antagonists. Indeed, the developmental progression is a robustly quantifiable bioassay that resolves MOD-1 activation by quipazine, 5-carboxyamidotryptamine and fluoxetine and highlight methiothepin as a potent antagonist. This assay has the intrinsic ability to highlight compounds with optimal bioavailability and furthermore to filter out off-target effects. It can be extended to the investigation of other classes of membrane receptors and modulators of neuronal excitation. This approach based on heterologous modulation of the essential M4 neuron function offers a route to discover new effective and selective anthelmintics potentially less confounded by disruptive environmental impact.

1. Introduction

Nematodes are an important class of disease causing organisms impacting human, animal and plant health. Approximately 24% of the global human population suffer from parasitic helminth infections (Garcia-Bustos et al., 2019) and it is estimated that damage caused by plant parasitic nematodes result in a $>$ 12% loss in global crop productivity (Abd-Elgawad and Askary, 2015). To express parasitism, nematodes use precise co-ordination of their behaviours to facilitate and sustain a life cycle that infects their host. This leaves these organisms susceptible to mitigating chemical treatments, i.e., nematicides and anthelmintics, that disrupt nervous system function and used in crop protection, veterinary and human medicine (Kimber and Fleming, 2005; Wolstenholme, 2011; Moreno et al., 2021). Although the nervous systems of nematodes are anatomically simple, they share a number of common molecular determinants with other organisms. This results in selective toxicity, in which chemicals that disrupt the parasite, are compromised by cross sensitivity of the host that is being treated (Nixon et al., 2020). The control of parasitic nematodes presents two distinct key challenges. One is to avoid detrimental consequences on the host. The second is off-target effects in other beneficial species (Dey et al., 2018). These confounds are compounded by the issue of emerging resistance in nematodes to anthelmintic agents in the face of widespread and persistent use (Kotze et al., 2020). To achieve the most effective parasite protection, ideal strategies need to be based on disruption of discrete, preferably species specific, pharmacological properties of

* Corresponding author.
E-mail address: F.Calahorro@soton.ac.uk (F. Calahorro).

https://doi.org/10.1016/j.pestbp.2022.105152
Received 28 February 2022; Received in revised form 18 May 2022; Accepted 16 June 2022
Available online 20 June 2022

nematode signalling molecules (Tyagi et al., 2019).

Selective chemical or drug action against parasitic nematodes can be achieved by targeting common signalling pathways as long as the nematode drug target harbours molecular features that engender species selective drug binding sites. The acetylcholine receptor agonist that selectively activates the L-type nicotinic receptor expressed at the body wall muscles of nematodes, levamisole, is an example of such an approach (Hernando et al., 2012; Lewis et al., 1980a; Lewis et al., 1980b). Additional chemicals that discretely impact neuronal targets include ivermectin and emodepside. Ivermectin acts on the glutamate-gated chloride receptor (GluCl) that is only found in invertebrates, and that harbours the binding site for ivermectin (Dent et al., 1997). This inhibits neuronal signalling and renders nematodes unviable thus breaking the nematode life cycle with limited detrimental effect on the mammalian host (Dent et al., 1997; Vassilatis et al., 1997; Cully et al., 1994). Emodepside activates calcium and voltage-dependent potassium channels that also inhibits neural signalling and muscle function to exert an anthelmintic action (Guest et al., 2007) that is apparently selective because of a differential sensitivity of the nematode and mammalian ion channel (Crisford et al., 2020).

Both levamisole and ivermectin target distinct classes of the cys-loop ligand-gated receptor superfamily. These receptors are built on a core structure in which five receptor subunits make a functional ligand-gated ion channel. The individual subunits have sequence divergence which allows them to express distinct molecular determinants essential to receptor function including agonist and antagonist binding. Interestingly, members of the cys-loop super-family are phylogenetically ancient and widely used as neurotransmitter receptors underpinning nervous system function in invertebrates (Lynagh and Lynch, 2012; Jaiteh et al., 2016). These include receptors that are divergent in sequence and suggest the possibility of the presence of pharmacophores unique to the parasitic nematodes (Raymond-Delpech et al., 2005; Jaiteh et al., 2016). For many of these receptors their agonists may be predicted by 'signature' amino acid sequences in the receptor protein found in the region of their agonist binding sites. However, many predicted receptor subunits have lost these signatures but still bind agonist (Tasneem et al., 2005) whereas others are presented as orphan receptors of unknown endogenous ligand. This raises the potential to make use of this poorly described pharmacology to identify new chemicals with excellent potential to endow the desired selective toxicity for novel approaches for nematode control (Peden et al., 2013).

MOD-1 is a member of a sub-group of the cys-loop family of ion channels that are activated by the biogenic amine 5-hydroxytryptamine, 5-HT. The MOD-1 receptor is a ligand-gated anion channel in contrast to the closest mammalian homologue which is the 5-HT_3 sub-class of receptor that is a ligand-gated cation channel (Ranganathan et al., 2000; Yuan et al., 2016). In nematodes, MOD-1 is structurally related to a group of other potential biogenic amine receptors for which only two have candidate endogenous agonists. *C. elegans* strains harbouring mutations in mod-*1* suggest that this plays important roles in nematode behaviours (Flavell et al., 2013). Although there is limited pharmacology, these receptors are sensitive to the 5-HT antagonist methiothepin (Ranganathan et al., 2000). As plant parasitic life cycle nematodes are susceptible to inhibition by the antagonist methiothepin (Crisford et al., 2020), this raises the intriguing potential for these receptors as an attractive target for chemical control of parasitic nematodes.

Screening approaches that facilitate the discovery of ligands for invertebrate ion channels are challenging (Yu et al., 2016). Efficient heterologous expression of invertebrate receptors often needs supporting co-expression of chaperones and other factors to drive receptor biogenesis (Boulin et al., 2008). This can be done by individually co-expressing these trafficking and chaperone proteins. A route to circumvent this is the heterologous expression of nematode receptors within the nematode organism but within cell types in which they are not physiologically expressed (Law et al., 2015). When the receptor is experimentally expressed in the tissue it makes it susceptible to application of an extrinsic molecule, that activates the ectopically expressed receptor. If this is coupled to an observable response it can provide the basis for a bioassay of receptor activation (Crisford et al., 2020). This approach underpins pharmacogenetic approaches that have been widely used to discretely regulate and explore circuit function in particular cells or model organisms (Law et al., 2015). This idea has also been developed with the view to using *C. elegans* behavioural read-outs to provide an approach for drug screening (Komuniecki et al., 2012; Law et al., 2015).

Here, we have developed a whole organism screening approach in *C. elegans* based on selectively targeting the essential pharyngeal neuron M4 pivotal in the worms pharyngeal function that underpins feeding. Laser ablation of M4 in early development identified it as the only pharyngeal neuron that was absolutely required for *C. elegans* to fully complete its development to an adult worm (Avery and Horvitz, 1987). Based on the limited phylogenetic distribution of *mod-1*, it has the potential to selectively disrupt nematode phyla. Further, we show that heterologous and ectopic expression of *C. elegans* or parasitic nematode, *Globodera pallida*, *mod-1* in M4 allows a pharmacogenetic activation that phenocopies M4 ablation. This targeted pharmacogenetic activation of M4 can be achieved in liquid cultures to generate a bioassay with quantitative fluorescent read-outs capable of identifying MOD-1 agonists and antagonists. We use this to provide a preliminary pharmacological profile for MOD-1 which identifies quipazine as an agonist. This study reveals that the PharmacoGenetic targeting of M4, or the so called PhaGeM4 approach, provides a route to defining MOD-1 modulating chemicals to serve as effective and selective agents for the control of parasitic nematodes. The underpinning rationale for this approach can be extended to other targets of interest if they can also be expressed in M4 to disrupt its function when activated.

2. Materials and methods

2.1. Phylogenetic analysis

We first used BLAST (Altschul et al., 1997) to identify protein sequences closely related to *C. elegans* MOD-1 in selected nematodes, arthropods and mammals, and then built phylogenetic trees based on the results. We also included examples of all major groups of the Cys-loop superfamily of receptors in the analysis. The indicated protein sequences were aligned using MEGAx (Molecular Evolutionary Genetics Analysis) (Stecher et al., 2020; Kumar et al., 2018) incorporating the MUSCLE algorithm (*multiple sequence alignment by log-expectation*). This processing was done with the following gap penalties using UPGMA as cluster method: gap open of −2.90 and hydrophobicity multiplier of 1.20, used as default parameters. The alignment outcome and the phylogenetic analysis was run using Maximum Likelihood statistical methods with a Jones-Taylor-Thornton (JTT) substitution model with a number of 500 bootstrap replications, and applying Nearest-Neighbor-Interchange (NNI) heuristic method for tree interference. Newick format outputs generated from phylogenetic assemblies were visualized using iTOL (interactive tree of life) v5.5 (EMBL-EBI) (Letunic and Bork, 2019).

The following protein sequences were used as input for the phylogenetic analysis: NP_741580.1 (MOD—1*C. elegans*); ADM53350.1 (MOD—1*H. contortus*); A0A183CI37 (GPA-MOD-1 *G. pallida*); XP_002637422 (CBR-MOD-1*C. briggsae*); EGT39436.1 (CBN-MOD-1C. *brenneri*); PIC27944.1 (CNI-MOD-1*C. nigoni*); A0A044RHY7 (OVO-MOD-1 *O. volvulus);* PDM74974.1 (MOD-1 *P. pacificus*); XP_003097605.1 (CRE-MOD-1*C. remanei*); CRZ21760.1 (BMY-MOD-1 *B. malayi*); EYC10594.1 (ACEY-MOD-1 *A. ceylanicum*); NP_501715.1 (ACC—1*C. elegans*); NP_501567.1 (ACC—2*C. elegans*); NP_508810.2 (ACC—3*C. elegans*); NP_499789.1 (ACC—4*C. elegans*); NP_498437.2 (ACR—5*C. elegans*); NP_509745.2 (ACR—8*C. elegans*); NP_505207.1 (ACR—16*C. elegans*); NP_001023961.1 (ACR—17*C. elegans*); NP_001122627.1 (ACR—20*C. elegans*); VDJ63109.1

(ACR—21*C. elegans*); NP_001317822.1 (ACR—23*C. elegans*); NP_001020962.1 (AVR-14*C. elegans*); NP_001024077.1 (AVR-15*C. elegans*); NP_001255705.1 (LEV-1*C. elegans*); NP_509932.2 (LEV-8*C. elegans*); NP_507870.2 (LGC-55*C. elegans*); NP_001023766.1 (LGC-36*C. elegans*); NP_499662.2 (LGC-37*C. elegans*); NP_507090.1 (GluCl-alpha *C. elegans*); NP_505897.1 (DEG—3*C. elegans*); NP_001256320.1 (DES—2*C. elegans*); NP_499661.2 (GAB—1*C. elegans*); NP_495229.3 (EXP-1*C. elegans*); NP_507090.1 (GLC-1*C. elegans*); VTW47520.1 (GGR-2*C. elegans*); ADN33421.1 (ACR-5H *H. contortus*); ADN33424.1 (ACR-17H *H. contortus*); ADN33426.1 (ACR-24H *H. contortus*); NP_001163656 (GluClalpha isoform K *D. melanogaster*); NP_650827.3 (GluClalpha isoform M *D. melanogaster*); AAF56303.1 (nAChRalpha2 isoform B *D. melanogaster*); AAF46361.3 (nAChRalpha3, isoform B *D. melanogaster*); AAF45409.3 (nAChRalpha4, isoform E *D. melanogaster*); NP_001356885.1 (nAChRalpha5, isoform I *D. melanogaster*); AAS64671.1 (nAChRalpha6, isoform E *D. melanogaster*); NP_001162795.1 (nAChRalpha7, isoform E *D. melanogaster*); NP_524483.1 (nAChRbeta2, isoform A *D. melanogaster*); NP_525098.1 (nAChRbeta3 *D. melanogaster*); XP_017847491.1 (GluCl *D. busckii*); NP_001071277 (GluCl *A. mellifera*); AJE70260.1 (nAChRa2 *A. mellifera*); NP_001073029.1 (nAChRa3 *A. mellifera*); NP_001091691.1 (nAChRa4 *A. mellifera*); AJE70263.1 (nAChRalpha5 *A. mellifera*); XP_026302163.1 (nAChRa6A isoform X6 *A. mellifera*); XP_026300655.1 (nAChRa7 isoform X1 *A. mellifera*); NP_001091694.1 (nAChRa9 *A. mellifera*); NP_001091699.1 (nAChRb2 *A. mellifera*); XP_031367920.1 (GABARbeta *A. dorsata*); NP_032095.1 (GABRB1 *M. musculus*); XP_011240700 (Htr3a *M. musculus*); CAA76154.1 (CHRNA2 *H. sapiens*); AAB40110.1 (CHRNA3 *H. sapiens*); AAB40111.1 (CHRNA4 *H. sapiens*); AAB40112.1 (CHRNA5 *H. sapiens*); AAB40113.1 (CHRNA6 *H. sapiens*); AAB40114.1 (CHRNA7 *H. sapiens*); AAM74523.1 (CHRNA9 *H. sapiens*); AAB40115.1 (CHRNB2 *H. sapiens*); AAB40116.1 (CHRNB3 *H. sapiens*); NP_000797.2 (GABRA1 *H. sapiens*); NP_001155244.1 (HTR3A *H. sapiens*).

2.2. Harvesting C. elegans embryos

Embryo isolation was performed as described (Strange et al., 2007) with some modifications. ~15 5.5 cm NGM plates containing approximately 600 gravid adults (L4 + 24–30 h-old) were washed by adding 2 ml of sterile ddH_2O. The washed worms were collected into a 15 ml conical sterile tube before being pelleted by centrifugation for 3 min at 1200 rpm. After removing the supernatant, the pellet was resuspended and washed twice by 5 ml of sterile ddH_2O, in order to remove the excess of bacteria. Worms were pelleted between washes by centrifugation for 3 min at 1200 rpm. The washed pellet was lysed using 2.5 ml of 12% alkaline hypochlorite solution in 1.6 M NaOH with continued vigorous manual shaking for exactly 4 min. The lysis was halted by the addition of 5 ml of autoclaved egg buffer (final concentration of 25 mM HEPES, 118 mM NaCl, 48 mM KCl, 2 mM $CaCl_2$, 2 mM $MgCl_2$) followed by centrifugation for 3 min at 1200 rpm. The wash was repeated before the released egg pellet was resuspended by mild agitation in 2.5 ml of ddH_2O. 2.5 ml sterile 60% sucrose (*W/V*) was carefully added below eggs and this was step was centrifuged for 1 min at 1200 rpm. Approximately 3 ml of the sucrose step harbouring the embryos was transferred into a fresh sterile 15 ml conical tube and washed with 5 ml of ddH_2O and centrifuged for 6 min at 1200 rpm. After two further washes the isolated egg pellet was resuspended in 100 μl of sterile ddH_2O. Three 1 μl aliquots were transferred onto agar plates and the number of eggs counted using a binocular dissecting microscope (Nikon SMZ800). This protocol usually identified 90–100 embryos per μl equivalent to 10,000 embryos per egg suspension. The viability/fertilization of these preparations was routinely checked by platting 30 eggs onto NGM (Nematode Grow Medium) with *E. coli* OP50 and their development monitored by visual inspection at 24–48 h at 20 °C. The appearance of L1-L2 larvae over this period indicated 90–95% of the isolated eggs were competent to express full development.

2.3. C. elegans strains and culture conditions

The culturing and maintenance of *C. elegans* were as previously described (Brenner, 1974). Monoxenic cultures of *C. elegans* embryos in S Medium based liquid cultures were largely as described (Lewis and Fleming, 1995). 3 ml of *E. coli* OP50 (OD_{600} of 0.8 AU) was pelleted and resuspended in completed S Medium (50 nM EDTA, 20 nM $FeSO_4.7H_2O$, 10 nM $MnCl_2.4H_2O$, 10 nM $ZnSO_4.7H_2O$, 1 nM $CuSO_4.5H_2O$, 0.013 mM cholesterol, 10 mM potassium citrate pH 6, 3 mM $CaCl_2$, 3 mM $MgSO_4$) to give a completed bacteria laced monoxenic culture. 50 μl of monoxenic culture was added into individual wells of a sterile Corning® 96-well microplate (Clear Flat Bottom Polystyrene) to support the development of *C. elegans* embryos. The increasing fluorescence through development was monitored from incubations made in sterile Grenier® 96-well microplates (f-bottom (chimney well) μclear®,black). Embryos suspensions at the indicated egg concentrations were deposited into individual wells. The microplate was covered from the light with foil, sealed by parafilm and gently agitated to facilitate oxygen circulation by constant orbital rotation (70 rpm).

Bristol N2 (wild type) and MT9668 mod-*1* (*ok103*) *V* x6 outcrossed strains were provided by CGC (*Caenorhabditis* Genetics Center, University of Minnesota). The worm strains made in this work are denotated as carrying *Caenorhabditis elegans* (Ce) or *Globodera pallida* (Gp) the following:

N2 (wt) sIs [P*myo-3*::*gfp*], N2 (wt) sIs [P*ceh-28*::*Cemod-1;* P*myo-3*::*gfp*] x3 outcrossed, N2 (wt) sIs [P*ceh-28*::*Gpmod-1;* P*myo-3*::*gfp*] x3 outcrossed, *mod-1 (ok103)* sIs [P*ceh-28*::*Cemod-1;* P*myo-3*::*gfp*] x3 outcrossed, *mod-1 (ok103)* Ex [P*myo-3*::*gfp*], *mod-1 (ok103)* Ex [P*mod-1*::*Cemod-1;* P*myo-3*::*gfp*], *mod-1 (ok103)* Ex [P*snb-1*::*Cemod-1;* P*myo-3*::*gfp*], *mod-1 (ok103)* Ex [P*myo-3*::*Cemod-1;* P*myo-3*::*gfp*].

N2 (wt) sIs [P*ceh-28*::*Cemod-1;* P*myo-3*::*gfp*] strain was used to perform experiments shown in Figs. 4, 5, 6 and 8. *mod-1 (ok103)* sIs [P*ceh-28*::*Cemod-1;* P*myo-3*::*gfp*] strain was used to perform experiments shown in Supplement 3 to Fig. 8.

2.4. Pharmacological drugs used

Serotonin hydrochloride (5-HT) (Merck-SigmaAldrich; CAS number: 153–98-0), 5-carboxyamidotryptamine maleate salt (5CT) (Merck-SigmaAldrich; CAS number: 74885–72-6), SR57227A (4-amino-1-(6-chloro-2-pyridil) piperidine hydrochloride) (Merck-SigmaAldrich; CAS number: 77145–61-0), quipazine (QPZ) (Merck-SigmaAldrich; CAS number: 5786-68-5), fluoxetine hydrochloride (FLOX) (Merck-SigmaAldrich; CAS number: 56296–78-7). All stocks that were used in the pharmacological experiments were made from powder, dissolved in water protected from light and added to experiment on the same day that stocks were prepared.

2.5. Cloning and transgenic methods

2.5.1. Cloning

The designated primer sequences were used to amplify genomic sequences harbouring the indicated promoters and these amplicons cloned into the pDEST expression vector pWormGate (Johnson et al., 2005): P*snb-1* (Fw 5′- CCAAGCTTTTTGCTGAAATCTAGG −3′; Rv 5′-TCCTCTAGAGCCGGCTGTTCCCTGAAATG −3′), P*myo-3* (Fw 5′-TCCTCTAGATGGATCTAGTGGTCGTGG −3′; Rv 5′-ACCAAGCTTGGGCTGCAGGTCGGCT −3′), Pmod-*1* (Fw 5′- TCGAGAAGCTTCATGTTTCACGGAACG −3′; Rv 5′- ACTACTCTAGAAATTTTCTTTCACC -3′), P*ceh-28* (Fw 5'-TCGAGGCATGCAATCTCTTATTACGAATATCAAAG −3′; Rv 5'-ACTACGGTACCTGGGACCACTAACTTCAAATTGTG −3′).

The cDNA sequences encoding the open reading frame of the *C. elegans* and *G. pallida* mod-*1* were amplified using the following primers: *FwCemod-1* 5′- ATGAAGTTTATTCCTGAAATCACAC -3′; *RvCemod-1* 5′- TCACTGATAGTTTTGATCGAAAC -3′; *FwGpmod-1* 5′-

GGTACCATGCTTTGCCCCAC -3′, *RvCemod-1* 5′- CTTAAGTTATTGTTTATTCGGAC -3′. DNA amplifications were carried out using both *C. elegans* cDNA template (OriGene) and *G. pallida* cDNA template using the Phusion High-Fidelity DNA Polymerase (Thermo Fisher Scientific) a following manufacturer instructions, briefly: initial denaturation of 30 s at 98 °C followed by following of 34 cycles consisting of 30 s at 98 °C, annealing 30 s at 58 °C, extension 40 s at 72 °C and a final extension 10 min at 72 °C.

MOD-1 sequences were cloned into the PCR™8/GW/TOPO® TA (Invitrogen™) vector, and individually recombined with the required PDEST vector harbouring the distinct promoters using Gateway™ LR Clonase™ reaction. The authenticity of the gDNA promoters and the cDNA sequences were verified by sequencing both strands of two independent clones using Sanger sequencing (Eurofins Genomics™).

2.5.2. Transgenic methods

Transgenic animals were generated by DNA microinjection as previously described (Mello et al., 1991). N2 (wt) and/or *mod-1* (*ok103*) *V* 1-day-old adults were microinjected with the indicated plasmids: P*snb-1::mod-1*, P*myo-3::mod-1*, P*mod-1::mod-1,* P*ceh-28::mod-1* (50 ng/μl) together with the 'marker' plasmid P*myo-3::gfp* (30 ng/μl). For controls, N2 (wt) or *mod-1* (*ok103*) animals were microinjected with 'empty rescue' plasmid and the marker plasmid P*myo-3::gfp* at the same concentration used to generate the rescue transgenic lines. Progeny from highly transmitting transformants (~90% segregation rate) were passaged and used to select experimental lines.

2.5.3. Integration of extrachromosomal arrays

15–20 fluorescent transgenic L4 animals from lines transmitting based on a cut-off of 80–90% segregation into the progeny, were picked onto unseeded culture plates. The uncovered plates were irradiated at 0.012 J/cm^2 for 2 s in a UV cross-linker (Stratagene UV stratalinker 1800). After irradiation animals were recovered for 12 h by incubation at 15 °C. To select potential integrated transgenic lines150–200 fluorescent F1 animals were grown onto individual culture plates. Four fluorescent transgenic F2s from each F1 plate were selected for high level of fluorescence and passaged. Populations that exhibited 100% inheritance were selected as homozygous integrants with successful integration. These selected integrants were outcrossed three times with Bristol N2 (wt) strain.

2.6. Imaging pharyngeal-pharmacological phenotypes

Modified NGM (Nematode Grow Media) omitting peptone and using agarose (Fisher, BP-100) instead agar was used to facilitate imaging by improving contrast. 1 ml of this molten 'imaging' media was dispensed into a 3 cm petri dish to generate a 1 mm thick arena and used within 24 h. To prepare drug laced NGM imaging plates, drug stocks were added at the indicated final concentration to tempered agar and the plates were stored away from light before use. In recovery experiments, the drug treated worms were removed from the drug containing agar plates and placed on a drug free OP50 lawn made up of 10 μl of *E. coli* at an OD_{600} of 0.8 AU. Individual animals were imaged using a Nikon Eclipse X microscope with a DIC optics using 40× Plan air objective. Images were acquired through a Hamamatsu Photonics camera and visualized for recording with IC-Capture© software (The Imaging Source©).

2.7. Behavioural assays

2.7.1. Pharmacological characterisation of the transgenic C. elegans strains in thrashing paralysis assay

Population based thrashing assays designed to assess the pharmacological effect of 5-HT on motility were conducted as described (Ranganathan et al., 2000). 10 to 20 animals (L4 + 1 day old), grown on OP50 NGM plates at 20 °C, were picked into individual wells of a sterile Corning® 96-well microplate (Clear Flat Bottom Polystyrene), containing 200 μl M9 buffer with or without 33 mM 5-HT. Thrashing behaviour was observed and counted (non-motile animals) every minute for a total time of 20 min under a binocular dissecting microscope (Nikon SMZ800). An animal was considered immotile if it did not exhibit any thrashing motion for a period of 5 s. To test whether methiothepin was able to block the 5HT-induced paralysis worms were pre-exposed with the indicated concentration of methiothepin (MT) by cultivating the worms on OP50 NGM plates for 120 min. The methiothepin dosed worms were subsequently transferred into the thrashing assay and dosed with 5-HT by adding stocks to reach the final indicated concentration.

2.7.2. Investigating pharyngeal pumping in MOD-1 expressing transgenic lines

To monitor the pharyngeal pumping activity of early developmental stages, synchronized gravid adults were transferred onto imaging plates (1 mm NGM with a thin OP50 lawn) to lay eggs. After 60–120 min of egg laying the original adult worms were removed. For the remaining observation of the distinct developmental stages were directly picked onto fresh imaging plates. Animals at the indicated developmental stage were identified by size and morphological landmarks (Uppaluri and Brangwynne, 2015) and incubated for 12 h in the presence of the indicated concentration of 5-HT. These were compared to age matched control worms incubated in the absence of 5HT. The worm pharyngeal pumping was video recorded for 30 s a Nikon Eclipse X microscope with a DIC optics (40× magnification). These recordings captured the coordinated pharyngeal contraction and relaxation based on the displacement of the grinder structure in the terminal bulb. One cycle of displacement and recovery of the grinder structure is counted as one pump. These video recordings were quantified for pump rate by an observer blind to the treatment. To monitor recovery of pharyngeal pumping in the 5-HT treated worms they were transferred onto a drug free agar plate for 5 min before finally placing them onto *E. coli* OP50 lawn without drug for 1, 2, 3, 5, 7 and 24 h. The total number of pumping events in individual animals was recorded at these indicated times. The pump rate was extracted from blinded video-recordings replayed by observer in slow motion (−0.5× frame-reproduction speed) to allow more precise estimates of observer-based pump rates.

2.7.3. Monoxenic culture embryos developmental assay

20 eggs from the indicated strain were dispensed into individual wells of 96-well microtiter plates containing 50 μl of monoxenic culture. An aliquot of 5-HT, QPZ, 5CT and SR57227 and FLOX drug stocks was added to the specified volume of monoxenic culture to the desired final concentration. The microtiter assay plates were protected from light. The eggs developed in the presence of the indicated concentration of drugs. As the embryos develop through L1 to L4 there is an increase in the GFP fluorescence driven by the co-expressed body wall muscle GFP. Thus, monitoring fluorescence from each well at 0, 24, 48 and 72 h using a FLUOstar microplate reader (BMG Labtech) provided a proxy for developmental progression. The microplate reader was set using the following parameters: gain 1000, bottom laser, 485 nm excitation – 528 nm emission wavelength.

2.8. Estimating the IC_{50} drug induced inhibition of developmental progression

The concentration of compound that caused a half maximal inhibition of developmental progression was calculated by non-linear regression of the concentration dependence of developmental arrest.

Worms were incubated in the absence or presence of increasing concentration of the indicated drugs and at 72 h the relative fluorescence associated with the worm population in each well was recorded. The fluorescence intensity of drug treated worms relative to the untreated worms was used to generate % maximum responses. This was plotted against drug concentration to generate a dose response curve

and converted to a sigmoidal dose-response curve of variable slope according to the following eq. Y = Bottom + (Top-Bottom)/(1 + 10^((LogAbsoluteIC50-X)*HillSlope + log((Top-Bottom)/(Fifty-Bottom)-1))) using Prism (GraphPad Prism version 5.00 for Mac OS X, GraphPad Software, San Diego California USA).

3. Results

3.1. MOD-1 is a homopentameric 5-HT gated chloride channel unique to the phylum Nematoda

MOD-1 and related biogenic amine and amino acid receptors are an under investigated class of ligand gated ion channels (Morud et al., 2021). In the case of MOD-1 there is a clear indication that they encode a receptor subunit that is capable of forming a functional homoligomeric anion channel (Ranganathan et al., 2000). The 5-HT dependent activation and the consequent 5-HT induced Cl^- influx executes important modulatory function. Relative to the other significant classes of inhibitory neurotransmitter gated ion channels this provides a unique modality in which a 5-HT pharmacophore couples to an inhibitory chloride influx. A phylogenetic analysis of MOD-1 places it in a discrete group that is exclusive to the nematode phylum, closely related to another class of the cys-loop superfamily, the *C. elegans* acetylcholine-gated chloride channels (ACCs), with LGC-55, an amine-gated chloride channel, sister to this grouping (Fig. 1A). MOD-1 is phylogenetically distinct from glutamate-gated chloride channels, and the related GABA and glycine receptors that underpin major inhibition in mammals and humans. Predictive protein folding modelling analysis indicates that *C. elegans*

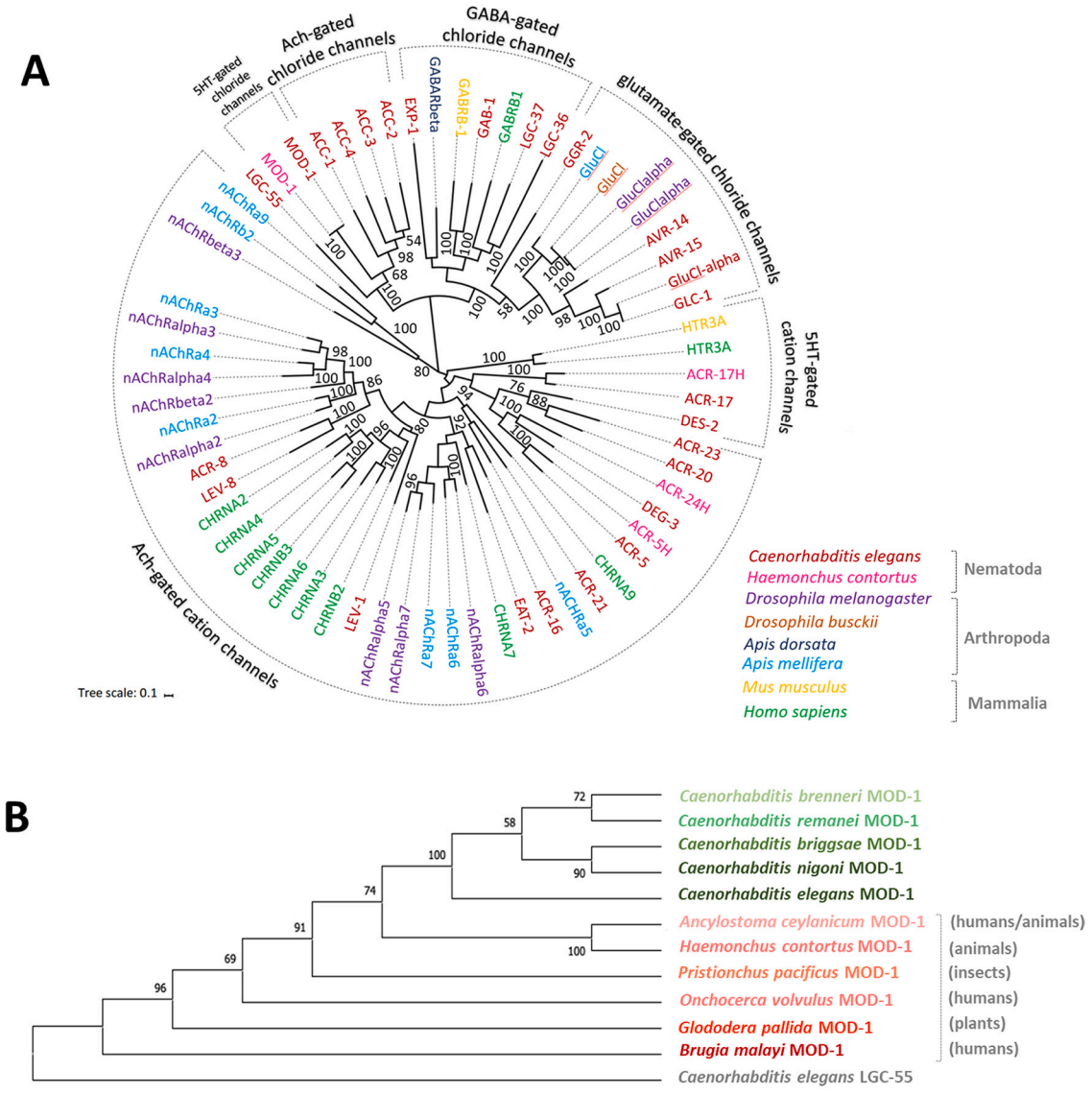

Fig. 1. Maximum likelihood phylogenetic tree of selected members of the Cys-loop superfamily of receptors.
A. The phylogenetic analysis of the major members of the Cys-loop receptor superfamily, discriminated MOD-1 from ACh−/5-HT gated cation channels and glutamate-/ACh-/GABA- gated chloride channel clusters. B. Phylogenetic representation of MOD-1 homologues in representative parasitic (red) and non-parasitic (green) species of nematodes, showing the conservation of this ion channel in the nematode phylum. The indicated host species for the listed parasites is shown in brackets.
The phylogenetic trees correspond to an evolutionary analysis inferred by Maximum Likelihood method JTT matrix-based model. The highest log likelihood values were − 65,525.00 and − 8232.73, for A and B respectively. The tree is drawn to scale, with branch lengths measured in the number of substitutions per site. Numbers on the nodes indicate the percentage of bootstrap supported for each node. (For interpretation of the references to colour in this figure legend, the reader is referred to the web version of this article.)

MOD-1 presents closest homology to crystalized known structures of other member of the cys-loop receptors superfamily. This is illustrated by the percentage of structural identity of ~30% with GABA receptor alpha subunit-1 of mammals (modelled by Swiss-Model, Swiss Institute of Bioinformatics). In addition, MOD-1 exists in both parasitic and non-parasitic nematodes (Fig. 1B). This phylogenetic relationship suggests conservation of MOD-1 channels between *Caenorhabditis* and other animal- and plant-parasitic nematodes (i.e., *Haemonchus contortus*, *Glododera* spp.).

3.2. Functional characterisation of MOD-1 5-HT receptor in C. elegans

In *C. elegans* a number of behavioural deficits in mod-*1 (ok103)* mutants have been identified supporting the contention that it has an important contribution to behaviour (Flavell et al., 2013). Moreover, *C. elegans mod-1* null mutants are resistant to the 5-HT induced paralysis observed in wild type animals. This paralysis is readily scored in a bioassay called thrashing in which the rate of flexing of individual worms can be counted. It has previously been reported that there is a dose dependent reduction in thrashing rate at high external concentrations (33 mM) of 5-HT (Ranganathan et al., 2000). In the first instance, we recapitulated this result and showed that the absence of 5-HT inhibition of thrashing in *mod-1(ok103)* could be reinstated by expression of wild-type *mod-1* from either the native promoter or a pan-neuronal promoter (*snb-1*) or a body-wall muscle promoter (*myo-3*), (Fig. 2). Thus, ectopic expression of the MOD-1 chloride channel can confer sensitivity to 5-HT.

These results highlight the value of ectopic expression as a route to a whole organism assay of receptor function. In view of the central role of feeding behaviour in driving *C. elegans* development we wanted to investigate if the feeding system could offer a route to developing a platform allowing the interrogation of MOD-1 pharmacology. In the first instance we expressed mod-*1* in the pharyngeal muscle to see if this non-native expression impacts on a feeding dependent assay. We observed that when we ectopically express the MOD-1 channel specifically into the pharyngeal muscles of *mod-1 (ok103)* mutants, this did not affect the pharyngeal pumping rate in presence of food (Fig. 3A). However, when we supplement the media 5-HT (10 mM) worms expressing MOD-1 in pharyngeal muscles had a severe inhibition of the pharyngeal pumping (Fig. 3B). Based on this, and the previous observation that ectopic

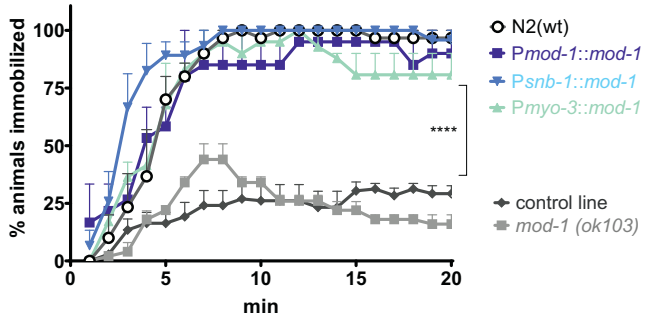

Fig. 2. mod-*1* dependent 5-HT paralysis is rescued by ectopic expression of *C. elegans mod-1* in body-wall muscles and neurons.
Native expression of *C. elegans mod-1* driven by *mod-1* promoter, and ectopic expression by both pan-neuronal (P*snb-1*) and/or body wall (P*myo-3*) muscle promoters in a *mod-1* (*ok103*) knock-out genetic background, confers sensitivity to paralysis to 33 mM 5-HT in the same manner as wild-type (N2) animals: P*mod-1*::*mod-1* vs *mod-1 (ok103)* / control line (**** $p \geq 0.0001$); P*snb-1*::*mod-1* / P*myo-3*::*mod-1*, vs *mod-1 (ok103)* (**** $p \geq 0.0001$). Control line indicated *mod-1 (ok103)* transgenic animals carrying the transgene P*myo-3*::*gfp* used as co-injection marker. Three stable lines for each transgenic strain were tested and the data are pooled. Data are shown as mean ± s.e.m. of animals immobilized; $n = 3$–5 independent experiments with a total number of 30–50 animals; two-way ANOVA with Bonferroni's multiple comparisons.

expression of MOD-1 effectively inhibits neuromuscular function, we considered ectopic expression as a platform for screening MOD-1 pharmacology.

3.3. Activation of MOD-1 in M4 neurons mediates inhibition of pharyngeal pumping

It has been established that the pharyngeal motor neuron M4 is the only essential neuron for feeding (Avery and Horvitz, 1987). Cholinergic transmission from M4 activates the isthmus peristalsis essential for the transport of food from corpus to the terminal bulb. Ablation of this cholinergic neuron behaviour essentially prevents feeding and leads to L1 arrest (Avery and Horvitz, 1987). This underpinned the rationale for our experimental approach in which MOD-1 was ectopically expressed selectively in the M4 neuron of *C. elegans*. This was achieved by making P*ceh-28* (Ray et al., 2008) transcriptional fusion containing the 5' UTR region of *ceh-28* and the protein encoding sequencing for MOD-1 (Fig. 4A). To select for the initial transgenics we used the transcription reporter P*myo-3*::*gfp* (Fig. 4A) that drove identifying expression in the body wall muscle. We generated stable lines of worms that expressed *mod-1* in the pharyngeal M4 neuron in that also carried GFP fluorescence in the body wall muscle (Fig. 4C). It is well characterized that the expression under the *ceh-28* 5′-upstream region is exclusive in M4 neuron from mid-embryogenesis (450 min post-first cleavage) through adult stages (Ray et al., 2008) (Fig. 4B).

We investigated the development of the resulting integrated line. This evidenced normal timeline of development when compared to the expected timings of N2 (wt) worms and contrasts to mutants with M4 feeding deficits such as *ceh-28* worms (Ray et al., 2008). Visual observation of the transgenic worms also identified an increasing body wall GFP signal derived by the co-integrated P*myo-3::gfp* marker. This increase relates to an increase in both the number of muscles cells and their volume as they develop and grow (Moerman and Fire, 1997; Moerman and Williams, 2006) (Fig. 4C). Using synchronized worms cultivated from embryo to adult allowed us to quantify the emergent GFP fluorescence during development and identify a non-saturated ~80 fold increase from 15 worms. These experiments were optimized for investigation in liquid and used in monoxenic culture (Fig. 4C). These data show that the transgene and the co-segregating reporter could be assayed in the context of a microtiter plate based monoxenic culture that would support assay handling and high-throughput screening.

The ablation of the pharyngeal M4 neuron leads to a loss of co-ordinated feeding. Interestingly, bacteria induced pumping is regulated by 5-HT via synaptic and volume transmission from ADF and NSM sensory neurons (Song and Avery, 2013). The fact that ectopic expression of MOD-1 in M4 neuron was not impacting on growth, suggests that endogenous 5-HT was not activating the ectopically expressed MOD-1 or its activation was insufficient to drive a neuronal inhibition that would be predicted if a 5-HT activated chloride channel was selectively expressed in the M4 neuron. We addressed this by investigating if exogenous 5-HT that would super exceed levels achieved endogenously, impacted on the food induced pumping that is essential for normal development (Fig. 5A). When food was supplemented with 10 mM 5-HT in N2 (wt) animals, they pumped at the same rate as wild type worms on a control food patch regardless of the developmental stage investigated. Interestingly, the L1 larvae showed a reduced basal pumping on food relative to the later developmental time consistent with a maturation of neuronal circuits for pharyngeal pumping during development. This is consistent with the fact that some synaptic branches of pharyngeal neurons such as NSMs are mostly absent at the L1 stage compared to the adult stage (Axang et al., 2008). Thus, the stimulation of feeding, pharyngeal pumping, that is caused by the presence of food, was not affected by exposure to 5-HT (Fig. 5B). In contrast, P*ceh-28*::mod-*1* transgenic animals across the different developmental stages showed an inhibited pharyngeal pumping in the presence of exogenous 5-HT (Fig. 5B). This was consistent with the exogenous 5-HT raising

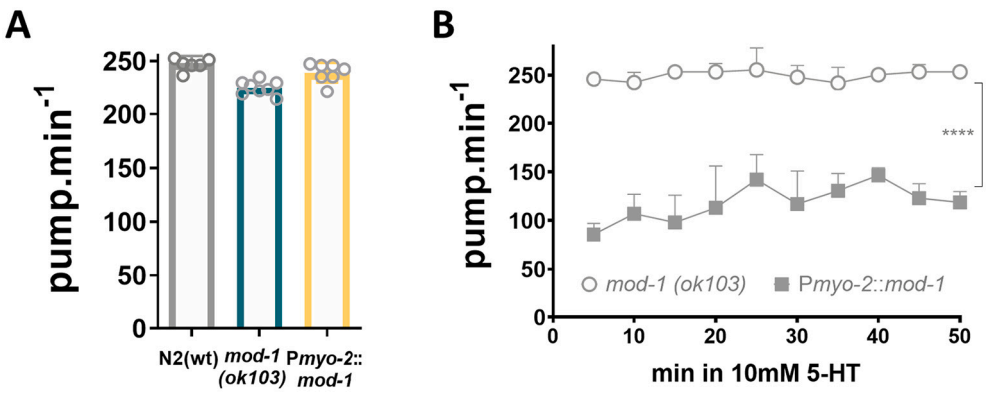

Fig. 3. *mod-1* ectopic expression in pharyngeal muscles promotes feeding inhibition.
A. The ectopic expression of the MOD-1 channel in pharyngeal muscles (P*myo-2*::*mod-1*) in *mod-1 (ok103)* mutants, has no significant detrimental effect on pharyngeal activity when feeding in presence of food. B. P*myo-2*::*mod-1* transgenic animals, feeding on food and in presence of 10 mM 5-HT, have a sustained reduction in the pharyngeal pumping rate.
Three stable lines for each transgenic strain were tested and the data are pooled. Data are shown as mean ± s.e.m. of pump.min^{-1}; n = 3 independent experiments with a total number of 7–10 animals. **** $p \geq 0.0001$; two-way ANOVA with Bonferroni's multiple comparisons.

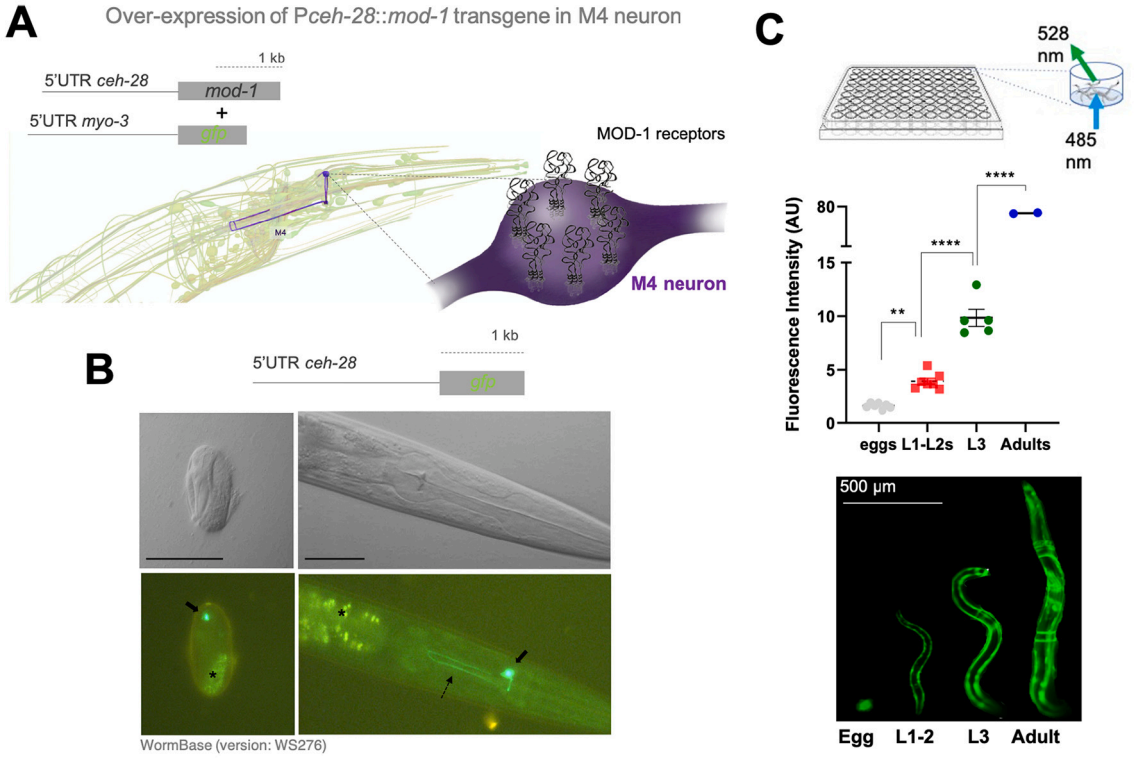

Fig. 4. Expression of the transgene P*ceh-28*::mod-*1* and Pmyo-3::*gfp* and fluorescence tracking of development.
A. Neuronal wiring modelling positioning the M4 pharyngeal neurons within the global worm's neuronal network using OpenWorm-WormBase simulation platform (http://openworm.org). A schematic representation of the over-expression of MOD-1 receptors (black) in a M4 cell body (violet) shown, as well as a diagram of the transgenes used to express *mod-1* in M4 neuron and the fluorescence marker *gfp* in body-wall muscle cells. B. The 5'UTR promoter region of *ceh-28* specifically drives expression in M4 neuron. The images represent bright field and epifluorescence views (top and bottom respectively) of the expression of a transcriptional reporter, expressing *gfp* driven by the 5'UTR *ceh-28* region specifically in M4 neurons during the very early stages of development as well as in the adult worm (Expression database, WormBase: WS276. Solid arrows point M4 cell body, dashed arrow points neuronal processes and the asterisks indicate autofluorescence signal. The scale bars indicate 50 µm). C. (Top) Schematic of monoxenic culture growth and relative fluorescence signal from 20 N2, P*ceh-28*::*Cemod-1*; P*myo-3*::*gfp* worms at indicated developmental stages grown in liquid monoxenic culture. C. (Bottom) Representative worms from the distinct stages of development from which population fluorescence is measured. This signal is proportional and correlates to each particular developmental stage. ** $p \geq 0.01$, **** $p \geq 0.0001$; one way ANOVA with Bonferroni's multiple comparisons. (For interpretation of the references to colour in this figure legend, the reader is referred to the web version of this article.)

internal 5-HT above the endogenous level available via food induced release, and this super-stimulus access the ectopically expressed MOD-1 dependent inhibition to generate a pharmacological ablation of M4 function. The selectivity of the MOD-1-5-HT mediated inhibition is evidenced by its reversal when 5-HT is removed (Fig. 5C) (Supplementary videos to Fig. 5).

To further characterize the dynamics of the ectopically induced MOD-1 dependent inhibition, we monitored the pharyngeal pumping, in a very early larvae stage (L1) after hatching in the absence of food but in presence of exogenous 5-HT. This was done by creating an imaging arena in which the pharyngeal pumping is directly monitored in the presence of 5-HT. Exposure of wild-type worms to 5-HT reduces motility facilitating the visualization of the pharynx and at the same time stimulates pharyngeal pumping (Fig. 6A). This showed the expected increase in pharyngeal pumping in N2 (wt) L1 5-HT treated worms. In contrast there was an initial, but blunted, increase in pumping in the P*ceh-28*::

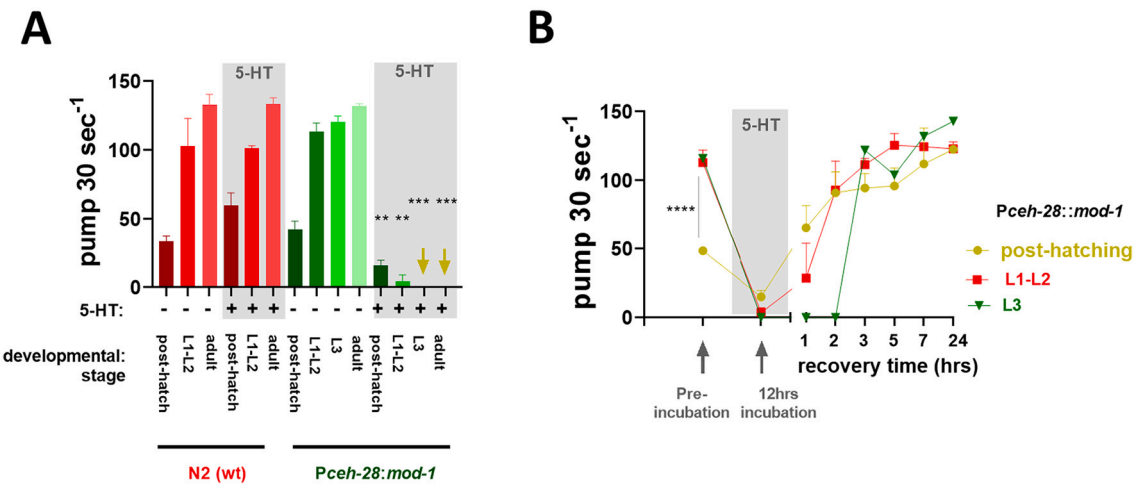

Fig. 5. Exogenous 5-HT inhibits the pharyngeal pumping in P*ceh-28*::*Cemod-1* transgenic animals across development.
A. The pharyngeal pump rate from N2 (wt) animals on food is the same at each of the stages tested when worms are assayed on food in the absence or presence of 10 mM 5-HT. Pharyngeal pumping of N2, P*ceh-28*::*mod-1* transgenic animals on food is selectively inhibited by the addition 10 mM 5-HT. B. 5-HT-dependent inhibition is reversible when worms are removed from 10 mM 5-HT. Data are shown as mean ± s.e.m. of animals in each particular developmental stage; $n = 3$ independent experiments with a total number of 3–7 (in A) 3–5 (in B) animals per concentration of 5-HT; two way ANOVA with Bonferroni's multiple comparisons (** $p \geq 0.01$, *** $p \geq 0.001$, ****$p \geq 0.0001$).

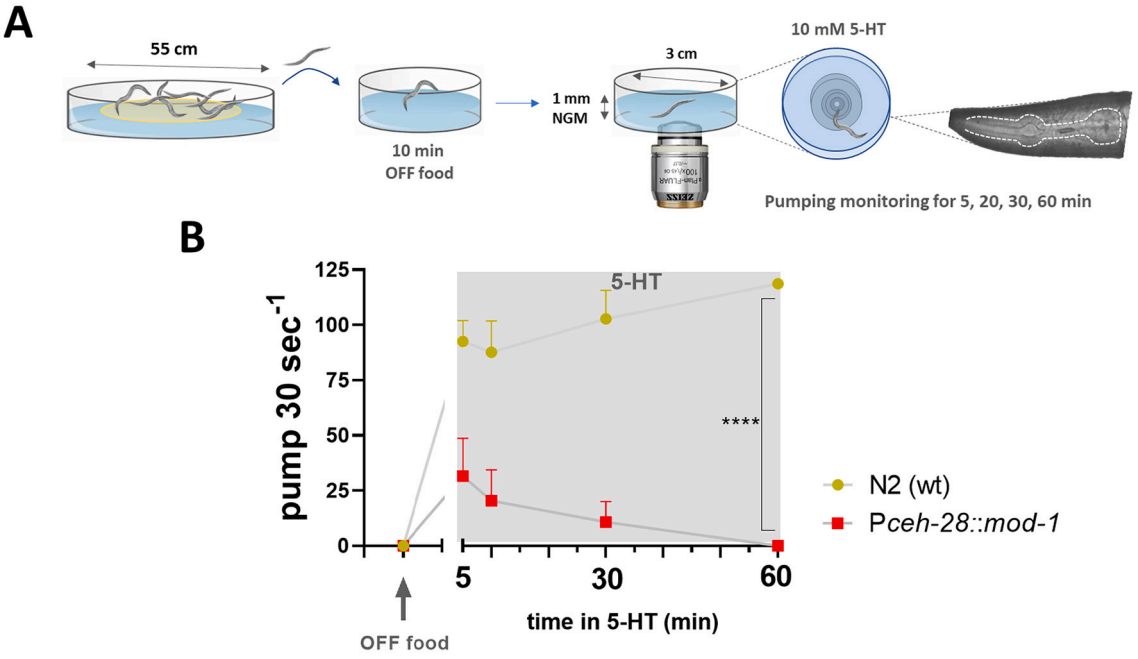

Fig. 6. Characterizing the time-course of the 5HT induced perturbation of pharyngeal pumping in the P*ceh-28*::*Cemod-1* transgenic animals.
A. Scheme depicting the workflow for the experiment and the transition from drug-free to 5-HT laced environments. Worms free of bacteria were transferred to plates with 5-HT and the pharyngeal pumping was monitored with a deep zoom (x63 optical magnification) for 5, 20, 30, 60 min. B. N2 (wt) elevates the pharyngeal pumping to the maximum basal level in presence of 10 mM 5-HT and N2, *Pceh-28*::*mod-1* transgenic animals showed a modest elevation in pumping that dissipates and is fully inhibited in the presence of 5-HT. Data are shown as mean ± s.e.m. of animals in each particular developmental stage; $n = 3$ independent experiments with a total number of 5–10 animals per concentration of 5-HT; two way ANOVA with Bonferroni's multiple comparisons (**** $p \geq 0.0001$).

mod-*1* animals. This was followed by complete inhibition of pumping in the continued presence of 5-HT (Fig. 6B). This observation is consistent with a preliminary activation of the 5-HT dependent stimulatory pathways coinciding with a slightly delayed inhibition mediated by the ectopically expressed *mod-1* in M4, and it reinforces the selective effect of the ectopically expressed mod-*1*.

3.4. Pharmacological activation of MOD-1 expressed in M4 neurons leads to developmental arrest in C. elegans

The data above highlight that the ectopic expression of *mod-1* provides a pharmacogenetic approach to acutely inhibit neuronal function in *C. elegans*. To relate this to earlier experiments in which neuronal ablation was able to prevent worm development, we monitored the development of the embryonic stage of P*ceh-28*::C*emod-1*/G*pmod-1* transgenic animals in the continued presence of 5-HT. In the absence of

5-HT normal development of the transgenic worms expressing *mod-1* in M4 was observed (Fig. 7). In contrast, when the food was supplemented with increasing doses of 5-HT there was an almost complete suppression of development and a marked reduction in the number of adults at 72 h (Fig. 7A, right panel). There was a threshold concentration of 5-HT for inhibition of development of around 0.1 mM. The inhibition of development was completely blocked by co-incubating with the MOD-1 antagonist methiothepin (10 μM) (Fig. 7A, B). Interestingly, methiothepin per se did not impact on the rate at which adults appeared, supporting the notion that the ectopically expressed mod-*1* is responsible for the effect.

To achieve granularity on this inhibitory effect of 5-HT on the development of worms expressing *mod-1* in M4, we investigated the proportion of distinct developmental stages that emerge from the synchronized embryo populations in untreated and 5-HT treated cultures. The number of L1 and L2 larvae that emerge with increasing time under control conditions show the expected progression of development marked by increasing proportions of the starting embryo population becoming L1 and L2. Importantly, methiothepin per se had no discernible effect of the development dynamic when assessed by this approach. In contrast, we saw a concentration dependent inhibition of developmental expression of the transgenic lines expressing either the *C. elegans* or the *G. pallida mod-1* in M4 neuron (Fig. 7A, B). At the highest doses of 5-HT the developmental arrest was equivalent to an L1 arrest of the whole population. However, at decreasing lower concentrations of 5-HT allowed more of the population to progress through development. In a similar way pre-incubation with the methiothepin preincubation with 5-HT inhibition prevented the 5-HT reversed this induced developmental arrest in the worms carrying the ectopically expressed MOD-1 receptor.

The above showed that the pharmacological modulation of the ectopically expressed P*ceh-28*::mod-*1* animals create a platform to investigate the sensitivity of the receptor and utilize the abrupt change in development as a selective and readily tractable bioassay. A limitation of this approach is the reliance on monitoring and drug dosing in an agar plate formats. We sought to circumvent this to facilitate faster throughput screening platform by growing transgenic animals in liquid using monoxenic culture in a multi-well format. We investigated whether the integrated GFP array could act as a surrogate for development of the worms i.e., by providing a quantitative fluorescent read-out of developmental progression. Thus, in this liquid phase platform we

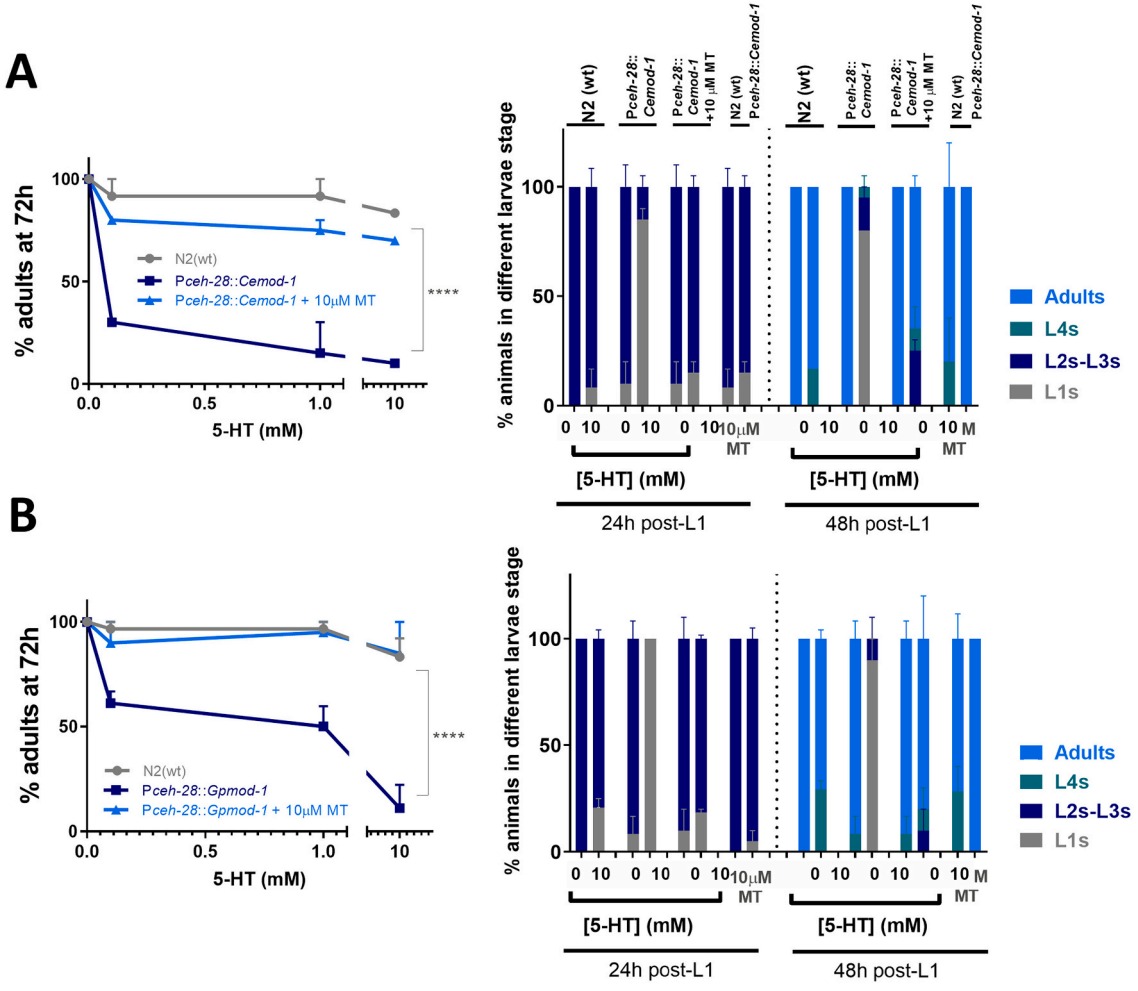

Fig. 7. Expression of *C. elegans* and *G. pallida* MOD-1 in the pharyngeal neuron M4 induces a 5-HT dependent developmental arrest.
The presence of 5-HT during the development of wild-type animals ectopically expressing (A) *C. elegans* or (B) *G. pallida* MOD-1 in M4 neuron inhibits feeding behaviour and causes subsequent larvae arrest. The left-hand panels show the proportion of adult animals after 72 h post-hatching incubation across the different experimental comparisons. This compares N2(wt) with P*ceh-28*::*Cemod-1* or P*ceh28*::*Gpmod-1* pre-incubated in increasing concentrations of 5-HT with, and without, 10 mM methiothepin. The transgenic expression of both *C. elegans* and *G. pallida mod-1* reduced the number of adults and showed a significant developmental arrest. The right-hand panels show a detailed track of development post hatching in the presence of 5-HT, indicating the cumulative proportion of different larvae stages at the indicated times. The presence of methiothepin per se at the concentration indicated showed no effect on development on N2(wt) or P*ceh-28*::*mod-1* animals (represented in the two more distal bars on the left-half of the graphs). Data are mean ± s.e.m. of animals at each developmental stage; $n = 3$ independent experiments with a total number of 30 animals per concentration of 5-HT; two-way ANOVA with Bonferroni's multiple comparisons (**** $p \geq 0.0001$).

monitored worm development based on the level of fluorescence emitted by P*ceh-28*::*mod-1* transgenic animals carrying the integrated P*myo-3*::*gfp* array in a N2 (wt) genetic background. As described above, this had no effect per se on *C. elegans* development (Fig. 4C). Using this format and varying numbers of starting embryos we optimized good sensitivity when 20 embryos are incubated in monoxenic culture in the absence of exogenous drug. This was evidenced by a clear time-dependent increase in GFP fluorescence. In keeping with previous observations, parallel incubations in the presence of food in monoxenic culture with 5-HT, showed a dose dependent inhibition of GFP fluorescence, consistent with the predicted MOD-1 mediated inhibition of M4 function, associated inhibition of feeding and developmental retardation. At the highest concentrations of 5-HT tested we saw that GFP remained at levels associated with the expression of the early egg encased embryo, consistent with a complete L1 arrest (Fig. 8A). This view is reinforced by visual inspection of the well contents after 72 h incubation that define all of the starting population are in the L1 stage. This developmental inhibition was reversed after removal of 5-HT and the development was resumed allowing the progression through the adulthood stages (Supplement 1 to Fig. 8). In the situation where there is a lower dose of 5-HT the GFP fluorescence shows a consistent increase in fluorescence but less than the controls not expressing mod-*1*. In addition, we developed an integrated transgenic line N2, P*myo-3*::*gfp* that can be use as control and reference of the GFP signal dynamic across development in wild type animals. We showed that both strains P*myo-3*::*gfp* and P*ceh-28*::mod-*1*; P*myo-3*::*gfp* develop in a similar manner in the absence of supplementing 5-HT. Furthermore the 5-HT inhibition of development observed was specifically dependent on the P*ceh-28*::*Cemod-1* transgene (Supplement 2 to Fig. 8).

As highlighted, the selective response of the P*ceh-28*::*mod-1* worms to exogenous 5-HT, in the face of endogenous release triggered by food, suggests that synaptically released 5-HT does not reach the concentration required to trigger ectopically expressed MOD-1. We investigated the pharmacological manipulation of endogenous levels of 5-HT via blockade of the 5-HT transporter with fluoxetine. Fluoxetine is a selective 5-HT reuptake inhibitor, leading to increased endogenous 5-HT concentrations in the synaptic cleft (Magni et al., 2013; Fuller and Beasley Jr., 1991). Incubation with increasing concentrations of fluoxetine provides a potent inhibition of development as indicated by a reduction in GFP fluorescence that suggests that sustaining the extracellular levels of endogenous released 5-HT leads to activating of the ectopically expressed MOD-1 (Fig. 8E).

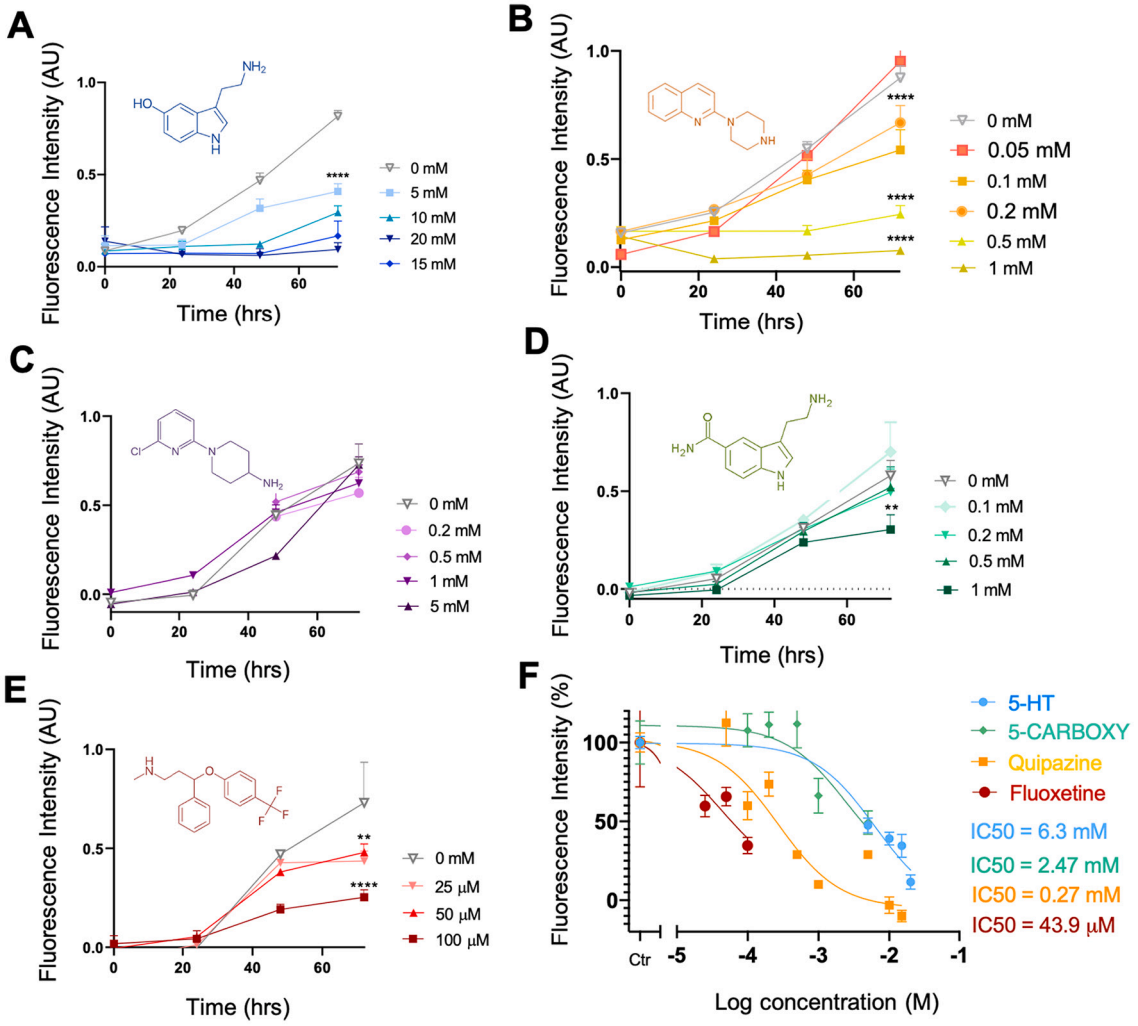

Fig. 8. Monoxenic culture bioassay for MOD-1 pharmacology.
Drugs with the indicated structures were added to individual wells of a 96 well microtiter plate each containing 20*C. elegans* embryos of N2, P*ceh-28*::*Cemod-1*; P*myo-3*::*gfp*. The fluorescence across time was measured in incubations made in the absence and presence of (A) 5-HT, (B) quipazine, (C) SR57227, (D) 5-carboxyamidotryptamine (E) and fluoxetine. (F) Comparison of IC_{50} curves obtained from measurements made at the 72 h incubation time. Data are shown as mean ± s.e.m. of normalised fluorescence intensity (AU) measured at 485 nm/528 nm (excitation/emission) at 0 h, 24 h, 48 h and 72 h time points; $n = 3$–7 independent experiments each containing about 20 worms per drug dose. Two-way ANOVA with Bonferroni's multiple comparisons (** $p \geq 0.01$; **** $p \geq 0.0001$).

In addition to testing the impact of indirect modulators of 5-HT bioavailability, we compared the relative potencies of some well characterized 5-HT agonists. To do this we compared compounds that have been used to activate and characterize the distinct classes of serotonergic receptors. In these experiments we observed that SR57227 (4-amino-1-(6-chloro-2-pyridil) piperidine hydrochloride) the selective 5-HT_3 receptor agonist had no observable effect at the concentrations tested. In contrast, both 5-carboxyamidotryptamine (5CT) and quipazine (QPZ) showed agonist dependent inhibition in developmental GFP accumulation. Interestingly, only QPZ was able to bring about the full inhibition also seen with 5-HT. This effect was consistent with complete L1 arrest as evidence by visual inspection of developmental stages. In contrast the more modest effect of 5CT coincided with more advanced stages of worm development (Fig. 8A–F) (Supplement 1 to Fig. 8). Similar effects of the tested drugs on development were observed when we used an integrated transgenic line P*ceh-28*::*mod-1;* P*myo-3*::*gfp* in a *mod-1 (ok103)* genetic background (Supplement 3 to Fig. 8). Utilizing PhaGeM4 as a proxy for receptor activity enabled us to estimate the IC_{50} value. This suggests a rank order of potency of QPZ > 5HT/5CT > SR57227.

4. Discussion

Our experiments rationalize MOD-1 as a candidate target for the development of novel chemical control of plant parasitic nematodes and as anthelmintics. We extend this by developing a bioassay in which *mod-1* is expressed in the essential neuron M4 of *C. elegans*. We extend this to a model hopping approach and show that *C. elegans* and parasitic orthologous of *mod-1* can be probed.

MOD-1 is a member of the cys-loop receptor superfamily that have an established role in organism selective toxicity via selective perturbation of parasitic nematode life cycle (Crisford et al., 2020). The possibility of utilizing the 5-HT receptors in nematodes as a target for pest control has been discussed and investigated in previous works (Komuniecki et al., 2012; Crisford et al., 2020). However, the challenge of wider use of 5-HT on these receptors is that the non-target organisms could also be affected. To this end, our work clearly demonstrates the presence of a nematode-specific 5-HT receptor, mod-*1* and this supports the development of a MOD-1-based platform which is potentially specific to the targeted parasite. Recent work has highlighted 5-HT controls key stages of hatching, plant invasion and plant location in the plant parasitic nematode *G. pallida* (Crisford et al., 2020). In particular, the methiothepin sensitivity of *G. pallida* hints at the potential for an involvement of the MOD-1 receptor.

In previous work, the molecular targets of chemicals that disrupt the nematode life cycle have been directly investigated using various model hopping approaches in *C. elegans* (Law et al., 2015). The experimental tractability of *C. elegans* and the increasing precision by which promoters can drive selective expression in distinct tissues and cell types can facilitate this process. In the context of 5-HT receptors this latter approach has identified that selective expression of 5-HT receptors, including MOD-1, can impart phenotypes and sensitivity to 5-HT receptor agonists (Law et al., 2015). In this study we showed that selective expression of *mod-1* in either body wall muscle or globally in neurons conferred a 5-HT dependent inhibition. Importantly, the *mod-1* orthologue of the receptor in parasitic *G. pallida* homology (Crisford et al., 2020), also conferred sensitivity to the inhibitory effect of 5-HT when ectopically expressed in muscle or neurons.

There are increasingly precise routes by which locomotion in liquid can be quantified with high throughput, including microtiter based formats. However, we were interested in developing throughput using an alternative approach based on viability. Previous work had established that the pharyngeal neuron M4 is critical for *C. elegans* development (Avery and Horvitz, 1987). This results from the activity dependent release of M4 acetylcholine that is fundamental in promoting feeding behaviour. This activity is dependent on 5-HT mediated excitation via SER-7 receptor (Song and Avery, 2013). Ablation at L1 larvae stage showed that the loss of M4 drives the loss of feeding and arrested growth. This, and another 5-HT dependent stimulation of MC neuron, increase feeding and are coordinated by an upstream food triggered release of pharyngeal 5-HT (Song and Avery, 2013). There is no evidence that mod-*1* is a determinant of this effect, and it is not expressed in any of the key pharyngeal structures that produce this critical feeding activation. We targeted M4 neuron with the ectopic expression of *mod-1* through the *ceh-28* promoter. An intermediary in this approach involved using the *myo-3* promoter that drives expression of the selection marker GFP in the body wall muscles. We noted that these transgenic worms expressing *mod-1* in M4 grew relatively normally on food. This is interesting as the 5-HT that is released by exposure of the worm to food would be available to activate the ectopically expressed MOD-1 which would ordinarily be expected to inhibit pumping. Our observations suggest that endogenous 5-HT in a physiological context is not activating MOD-1. In addition, monitoring growth and GFP fluorescence throughout development showed that increasing fluorescence could act as a proxy for population progression.

Experiments in which the food that drives pharyngeal pumping is supplemented with exogenous 5-HT showed that the pharynx of worms expressing MOD-1 in M4 was susceptible to 5-HT mediated inhibition of pumping, highlighting that exceeding the physiological levels of 5-HT was sufficient to execute a potent activation of the ectopically expressed MOD-1. This suggests that the affinity of the distinct 5-HT binding sites on the GPCR receptors that drive physiological pumping are at a higher affinity or more proximal to the synaptically released 5-HT than seen by MOD-1. Previous estimates of the EC_{50} of MOD-1 for 5-HT have been obtained from oocyte expression studies which benchmark it as around 1 μM (Ranganathan et al., 2000). However, the GPCRs have estimated EC_{50} values that are in the low nM range, supporting the notion that 5-HT is a more potent activator at the receptors that drive the physiological increase in pumping (Hobson et al., 2006). This would explain why the endogenous 5-HT mechanisms are preferentially activated in the absence of exogenous pharmacologically applied 5HT. This conclusion is reinforced by the observation that during the pharmacological application of exogenous 5-HT there is a transient increase in pumping that precedes the sustained inhibition mediated by the ectopic expression of mod-*1* in M4. As the accumulated levels of internal 5-HT are likely to increase with time, it supports the notion that the stimulatory effects are executed by lower concentrations of internal 5-HT than required to activate MOD-1. This assumption is further supported by the observation that the 5-HT reuptake inhibitor fluoxetine, that will pharmacologically elevate the ambient 5-HT, leads to an inhibition of the sustained pumping that is otherwise not seen in the presence of food alone. Thus, our data highlight that feeding behaviour could be regulated by ectopic expression of MOD-1, and this inhibition could be discretely activated at all stages of the pharyngeal life cycle when independently investigated as a consequence of 5-HT application. With the exposure of transgenic worms at L1 through to adult we were able to execute a MOD-1 dependent inhibition of pharyngeal pumping. This observation is consistent with classic ablation studies that identified and refined the view that M4 functions as a pivotal determinant of worm development (Avery and Horvitz, 1987). This lead to our investigation of whether MOD-1 induced arrested development could be used as a bioassay for MOD-1 agonists or modulators.

As indicated, the assay in a liquid handling format in microtiter plates engendered flexibility that increases the potential throughput of drug effects. Thus, we explored the use of development associated increase in GFP fluorescence from synchronized worm populations cultivated in liquid media. We optimized the number of embryos at the start of the assay to give a robust fluorescence which showed a ~ 80 fold increase during the time in which the added embryos went through development to the adult. In terms of identifying potency, our experiments showed that we were able to get almost complete inhibition of the increased GFP signal at the highest concentration of 5-HT tested in the

mod-*1* transgenic worms. Importantly, this was a dose dependent inhibition which suggests that the lower occupancy of the ectopic receptor expressed from the P*ceh-28*::*mod-1* transgene leads to a less than maximal inhibition of pumping. This is consistent with observation made on the impact of 5-HT on individually imaged worms and reinforced by the potent L1 arrest when populations were treated with maximal doses. This comparison supports the notion that assays based on the population response in culture provide a robust platform to assess the potency of candidate MOD-1 ligands.

To scope the potential of this approach we compared the efficacy of four distinct agonist structures. There is limited understanding of the structure/function relation of MOD-1 although mianserin and methiothepin have been identified as relatively potent antagonists (Sawin et al., 2000; Ranganathan et al., 2000). There are two types of distinct binding sites in 5-HT receptors. The first is that found in the structurally distinct class 1A GPCRs in which 5-HT like other biogenic amines adopts an extended structure and makes contacts with residues in the transmembrane domains of these receptors (Nelson, 1991). In contrast, the 5-HT binding in the ligand-gated ion channels like the 5-HT_3 and MOD-1 utilize the interface between two of the subunits in the homoligomeric receptor. Given this natural agonist, 5-HT and the commonly used analogue carboxyamidotryptamine (5CT) are known to have shared potency at both receptors, and our observation of the effect expressed by MOD-1 receptor are consistent with this. Interestingly, in view of the shared structural homology of MOD-1 and 5-HT_3 receptors, the lack of potency seen with exogenous application of SR57227 is striking. In contrast quipazine, a drug with similar physico-chemical characteristics, acts as the most potent of the compounds tested. Quipazine is a known 5-HT_3 receptor agonist, although it has clear potency at the mammalian 5-HT2C GPCR receptor consistent with the idea it imparts its action with key determinants in both ligand-gated and GPCR 5-HT binding sites. Recent structural studies of the 5-HT_3 receptor have identified critical contact residues in the 5-HT_3 binding site (Yuan et al., 2016; Kesters et al., 2013; Mu et al., 2003), and sequence alignment identifies canonical aromatic residues around loops B, C and D (Phe_{80}, Tyr_{180}, Tyr_{221}, Trp_{226}) that are conserved in the MOD-1 sequence. This analysis indicates that MOD-1 has a core 5-HT binding domain with sufficient deviation to impart potentially selective pharmacology that could be exploited for nematicide and anthelmintic development.

In conclusion, we highlight MOD-1 as a novel phylogenetically restricted target for nematode control (Law et al., 2015; Morud et al., 2021). This approach is likely useful to consider in the arena of human, animal and plant parasitic worms with the potential to improve selective toxicity, break drug resistance and reduce environmental impacts. To facilitate this, we have identified that ectopic expression of endogenous or parasitic nematode *mod-1*, in the essential feeding neuron M4 generates a platform for improved throughput screening. This assay offers a binary (developmental arrest and growth) and incremental readout of efficacy in liquid culture using GFP fluorescence to measure the drug effects. We show that the platform has the ability to identify agonists and antagonists. Not explored here, but worthy of consideration is the potential to identify chemicals that act as allosteric modulators. Given the value of phylogenetic selective agonists/antagonists and allosteric modulators in parasitic pest control, the PhaGeM4 assay will help approaches aimed at extending the utility of candidate targets and classes of chemicals capable of selectively targeting these.

Supplementary data to this article can be found online at https://doi.org/10.1016/j.pestbp.2022.105152.

Acknowledgements

We thank Professor Peter Urwin and Dr. Catherine Lilley (Centre for Plant Sciences, University of Leeds, UK) for their discussion and collaboration. F.C. and K.D. are supported by Biotechnology and Biological Sciences (BBSRC) grant number BB/T002867/1. Some *C. elegans* strains were provided by the CGC, which is funded by NIH Office of Research Infrastructure Programs (P40 OD010440).

References

Abd-Elgawad, M., Askary, T.H., 2015. Impact of phytonematodes on agriculture economy. In: Askary, T.H., Martinelli, P.R.P. (Eds.), Biocontrol Agents of Phytonematodes. CAB International Publishing, Oxfordshire, UK: Boston, MA, USA, pp. 12–17.

Altschul, S.F., Madden, T.L., Schäffer, A.A., Zhang, J., Zhang, Z., Miller, W., Lipman, D.J., 1997. Gapped BLAST and PSI-BLAST: a new generation of protein database search programs. Nucleic Acids Res. 25 (17), 3389–3402.

Avery, L., Horvitz, H.R., 1987. A cell that dies during wild-type *C. elegans* development can function as a neuron in a ced-3 mutant. Cell 51, 1071–1078.

Axang, C., Rauthan, M., Hall, D.H., Pilon, M., 2008. Developmental genetics of the *C. elegans* pharyngeal neurons NSML and NSMR. BMC Dev. Biol. 8, 38.

Boulin, T., Gielen, Marc, Richmond, Janet E., Williams, Daniel C., Paoletti, Pierre, Bessereau, Jean-Louis, 2008. Eight genes are required for functional reconstitution of the *Caenorhabditis elegans* levamisole-sensitive acetylcholine receptor. Proc. Natl. Acad. Sci. U. S. A. 105 (47), 18590–18595.

Brenner, S., 1974. The genetics of *Caenorhabditis elegans*. Genetics 77, 71.

Crisford, A., Calahorro, F., Ludlow, E., Marvin, J.M.C., Hibbard, J.K., Lilley, C.J., Kearn, J., Keefe, F., Johnson, P., Harmer, R., Urwin, P.E., O'Connor, V., Holden-Dye, L., 2020. Identification and characterisation of serotonin signalling in the potato cyst nematode *Globodera pallida* reveals new targets for crop protection. PLoS Pathog. 16 (10), e1008884 https://doi.org/10.1371/journal.ppat.1008884.

Cully, D.F., Vassilatis, D.K., Liu, K.K., Paress, P.S., Van der Ploeg, L.H., Schaeffer, J.M., Arena, J.P., 1994. Cloning of an avermectin-sensitive glutamate-gated chloride channel from *Caenorhabditis elegans*. Nature 371, 707–711.

Dent, J.A., Davis, M.W., Avery, L., 1997. avr-15 encodes a chloride channel subunit that mediates inhibitory glutamatergic neurotransmission and ivermectin sensitivity in *Caenorhabditis elegans*. EMBO J. 16, 5867–5879.

Dey, S., Luo, H., Fokoue, A., Hu, J., Zhang, P., 2018. Predicting adverse drug reactions through interpretable deep learning framework. BMC Bioinformatics. 19 (Suppl. 21), 476.

Flavell, S.W., Pokala, Navin, Macosko, Evan Z., Albrecht, Dirk R., Larsch, Johannes, Bargmann, Cornelia I., 2013. Serotonin and the neuropeptide PDF initiate and extend opposing behavioral states in *C. elegans*. Cell 154 (5), 1023–1035.

Fuller, R.W., Beasley Jr., C.M., 1991. Fluoxetine mechanism of action. J. Am. Acad. Child Adolesc. Psychiatry 30, 849.

Garcia-Bustos, J.F., Sleebs, B.E., Gasser, R.B., 2019. An appraisal of natural products active against parasitic nematodes of animals. Parasit. Vectors 12 (1), 306.

Guest, M., Bull, K., Walker, R.J., Amliwala, K., O'Connor, V., Harder, A., Holden-Dye, L., Hopper, N.A., 2007. The calcium-activated potassium channel, SLO-1, is required for the action of the novel cyclo-octadepsipeptide anthelmintic, emodepside, in *Caenorhabditis elegans*. Int. J. Parasitol. 37 (14), 1577–1588.

Hernando, G., Bergé, I., Rayes, D., Bouzat, C., 2012. Contribution of subunits to *Caenorhabditis elegans* levamisole-sensitive nicotinic receptor function. Mol. Pharmacol. 82, 550–560.

Hobson, R.J., Hapiak, V.M., Xiao, H., Buehrer, K.L., Komuniecki, P.R., Komuniecki, R.W., 2006. SER-7, a *Caenorhabditis elegans* 5-HT7-like receptor, is essential for the 5-HT stimulation of pharyngeal pumping and egg laying. Genetics 172 (1), 159–169.

Jaiteh, M., Taly, A., Hénin, J., 2016. Evolution of pentameric ligand-gated ion channels: pro-loop receptors. PLoS One 11 (3), e0151934.

Johnson, N.M., Behm, C.A., Trowell, S.C., 2005. Heritable and inducible gene knockdown in *C. elegans* using Wormgate and the ORFeome. Gene. 359, 26–34.

Kesters, D., Thompson, Andrew J., Brams, Marijke, van Elk, René, Spurny, Radovan, Geitmann, Matthis, Villalgordo, Jose M., Albert Guskov, U., Danielson, Helena, Lummis, Sarah C.R., Smit, August B., Ulens, Chris, 2013. Structural basis of ligand recognition in 5-HT3 receptors. EMBO Rep. 14 (1), 49–56.

Kimber, M.J., Fleming, C.C., 2005. Neuromuscular function in plant parasitic nematodes: a target for novel control strategies? Parasitology. 131 (Suppl), S129–S142.

Komuniecki, R., Law, W.J., Jex, A., Geldhof, P., Gray, J., Bamber, B., Gasser, R.B., 2012. Monoaminergic signaling as a target for anthelmintic drug discovery: receptor conservation among the free-living and parasitic nematodes. Mol. Biochem. Parasitol. 183 (1), 1–7.

Kotze, A.C., Gilleard, J.S., Doyle, S.R., Prichard, R.K., 2020. Challenges and opportunities for the adoption of molecular diagnostics for anthelmintic resistance. Int. J. Parasitol. Drugs Drug Resist. 14, 264–273.

Kumar, S., Stecher, G., Li, M., Knyaz, C., Tamura, K., 2018. MEGA X: molecular evolutionary genetics analysis across computing platforms. Mol. Biol. Evol. 35, 1547–1549.

Law, W., Wuescher, Leah M., Ortega, Amanda, Hapiak, Vera M., Komuniecki, Patricia R., Komuniecki, Richard, 2015. Heterologous expression in remodeled *C. elegans*: a platform for monoaminergic agonist identification and anthelmintic screening. PLoS Pathog. 11 (4), e1004794.

Letunic, I., Bork, P., 2019. Interactive tree of life (iTOL) v4: recent updates and new developments. Nucleic Acids Res. 47, W256–w259.

Lewis, J.A., Fleming, J.T., 1995. Chapter 1 basic culture methods. In: Epstein, H.F., Shakes, D.C. (Eds.), Methods in Cell Biology, vol. 48. Academic Press, pp. 3–29.

Lewis, J.A., Wu, C.H., Berg, H., Levine, J.H., 1980a. The genetics of levamisole resistance in the nematode *Caenorhabditis elegans*. Genetics 95, 905–928.

Lewis, J.A., Wu, C.H., Levine, J.H., Berg, H., 1980b. Levamisole-resistant mutants of the nematode *Caenorhabditis elegans* appear to lack pharmacological acetylcholine receptors. Neuroscience 5, 967–989.

Lynagh, T., Lynch, J.W., 2012. Molecular mechanisms of Cys-loop ion channel receptor modulation by ivermectin. Front. Mol. Neurosci. 7 (5), 60.
Magni, L.R., Purgato, M., Gastaldon, C., Papola, D., Furukawa, T.A., Cipriani, A., Barbui, C., 2013. Fluoxetine versus other types of pharmacotherapy for depression. Cochrane Database Syst. Rev. 7, 1–345. Cd004185.
Mello, C.C., Kramer, J.M., Stinchcomb, D., Ambros, V., 1991. Efficient gene transfer in *C. elegans*: extrachromosomal maintenance and integration of transforming sequences. EMBO J. 10, 3959–3970.
Moerman, D.G., Fire, A., 1997. Muscle structure, function and development. In: Riddle, D.L., Blumenthal, T., Meyer, B.J., Priess, J.R. (Eds.), *C. elegans* II. Cold Spring Harbor Laboratory Press, Cold Spring Harbor, NY, pp. 417–470.
Moerman, D.G., Williams, B.D., 2006. Sarcomere assembly in *C. elegans* muscle. In: WormBook. https://doi.org/10.1895/wormbook.1.81.1 ed. The C. elegans Research Community, WormBook.
Moreno, Y., Geary, T.G., Tritten, L., 2021. When secretomes meet anthelmintics: lessons for therapeutic interventions. Trends Parasitol. 37 (6), 468–475.
Morud, J., Hardege, I., Liu, H., Wu, T., Choi, M.K., Basu, S., Zhang, Y., Schafer, W.R., 2021. Deorphanization of novel biogenic amine-gated ion channels identifies a new serotonin receptor for learning. Curr. Biol. 31 (19), 4282–4292.e6. https://doi.org/10.1016/j.cub.2021.07.036.
Mu, T., Lester, Henry A., Dougherty, Dennis A., 2003. Different binding orientations for the same agonist at homologous receptors: a lock and key or a simple wedge? J. Am. Chem. Soc. 125 (23), 6850–6851.
Nelson, D.L., 1991. Structure-activity relationships at 5-HT1A receptors: binding profiles and intrinsic activity. Pharmacol. Biochem. Behav. 40 (4), 1041–1051. https://doi.org/10.1016/0091-3057(91)90124-k (PMID: 1816558).
Nixon, S.A., Welz, C., Woods, D.J., Costa-Junior, L., Zamanian, M., Martin, R.J., 2020. Where are all the anthelmintics? Challenges and opportunities on the path to new anthelmintics. Int. J. Parasitol. Drugs Drug Resist. 14, 8–16.
Peden, A.S., Mac, P., Fei, Y.J., Castro, C., Jiang, G., Murfitt, K.J., Miska, E.A., Griffin, J.L., Ganapathy, V., Jorgensen, E.M., 2013. Betaine acts on a ligand-gated ion channel in the nervous system of the nematode *C. elegans*. Nat. Neurosci. 16, 1794–1801.
Ranganathan, R., Cannon, S.C., Horvitz, H.R., 2000. MOD-1 is a serotonin-gated chloride channel that modulates locomotory behaviour in *C. elegans*. Nature 408, 470–475.
Ray, P., Schnabel, R., Okkema, P.G., 2008. Behavioral and synaptic defects in *C. elegans* lacking the NK-2 homeobox gene ceh-28. Dev. Neurobiol. 68, 421–433.
Raymond-Delpech, V., Matsuda, K., Sattelle, B.M., Rauh, J.J., Sattelle, D.B., 2005. Ion channels: molecular targets of neuroactive insecticides. Invertebr. Neurosci. 5 (3–4), 119–133.
Sawin, E.R., Ranganathan, R., Horvitz, H.R., 2000. C. elegans Locomotory rate is modulated by the environment through a dopaminergic pathway and by experience through a serotonergic pathway. Neuron 26 (3), 619–631.
Song, B., Avery, Leon, 2013. The pharynx of the Nematode *C. elegans*: a model system for the study of motor control. Worm 2 (1) e21833.
Stecher, G., Tamura, K., Kumar, S., 2020. Molecular evolutionary genetics analysis (MEGA) for macOS. Mol. Biol. Evol. 37, 1237–1239.
Strange, K., Christensen, M., Morrison, R., 2007. Primary culture of *Caenorhabditis elegans* developing embryo cells for electrophysiological, cell biological and molecular studies. Nat. Protoc. 2, 1003–1012.
Tasneem, A., Iyer, L.M., Jakobsson, E., Aravind, L., 2005. Identification of the prokaryotic ligand-gated ion channels and their implications for the mechanisms and origins of animal Cys-loop ion channels. Genome Biol. 6 (1), R4.
Tyagi, R., Elfawal, M.A., Wildman, S.A., Helander, J., Bulman, C.A., Sakanari, J., Rosa, B. A., Brindley, P.J., Janetka, J.W., Aroian, R.V., Mitreva, M., 2019. Identification of small molecule enzyme inhibitors as broad-spectrum anthelmintics. Sci. Rep. 9 (1), 9085.
Uppaluri, S., Brangwynne, C.P., 2015. A size threshold governs *Caenorhabditis elegans* developmental progression. Proc. Biol. Sci. 282 (1813), 20151283.
Vassilatis, D.K., Arena, J.P., Plasterk, R.H., Wilkinson, H.A., Schaeffer, J.M., Cully, D.F., Van der Ploeg, L.H., 1997. Genetic and biochemical evidence for a novel avermectin-sensitive chloride channel in *Caenorhabditis elegans*. Isolation and characterization. J. Biol. Chem. 272, 33167–33174.
Wolstenholme, A.J., 2011. Ion channels and receptor as targets for the control of parasitic nematodes. Int. J. Parasitol. Drugs Drug Resist. 1 (1), 2–13.
Yu, H.B., Li, M., Wang, W.P., Wang, X.L., 2016. High throughput screening technologies for ion channels. Acta Pharmacol. Sin. 37 (1), 34–43.
Yuan, S., Filipek, Slawomir, Vogel, Horst, 2016. A gating mechanism of the serotonin 5-HT3 receptor. Structure 24 (5), 816–825.